VOLUME 33 · NUMBER 34 · DECEMBER 1 2015

JOURNAL OF CLINICAL ONCOLOGY

BIOLOGY OF NEOPLASIA

Extreme Outlier Analysis Identifies Occult Mitogen-Activated Protein Kinase Pathway Mutations in Patients With Low-Grade Serous Ovarian Cancer

Rachel N. Grisham, Brooke E. Sylvester, Helen Won, Gregory McDermott, Deborah DeLair, Ricardo Ramirez, Zhan Yao, Ronglai Shen, Fanny Dao, Faina Bogomolniy, Vicky Makker, Evis Sala, Tara E. Soumerai, David M. Hyman, Nicholas D. Socci, Agnes Viale, David M. Gershenson, John Farley, Douglas A. Levine, Neal Rosen, Michael F. Berger, David R. Spriggs, Carol A. Aghajanian, David B. Solit, and Gopa Iyer

Rachel N. Grisham, Brooke E. Sylvester, Helen Won, Deborah DeLair, Zhan Yao, Ronglai Shen, Fanny Dao, Faina Bogomolniy, Vicky Makker, Evis Sala, Tara E. Soumerai, David M. Hyman, Douglas A. Levine, Neal Rosen, Michael F. Berger, David R. Spriggs, Carol A. Aghajanian, David B. Solit, and Gopa Iyer, Memorial Sloan Kettering Cancer Center; Rachel N. Grisham, Gregory McDermott, Vicky Makker, David M. Hyman, Neal Rosen, Michael F. Berger, David R. Spriggs, Carol A. Aghajanian, David B. Solit, and Gopa Iyer, Weill Cornell Medical College; Ricardo Ramirez, Graduate School of Medical Sciences; Nicholas D. Socci and Agnes Viale, Michael F. Berger, and David B. Solit, Marie-Josée and Henry R. Kravis Center for Molecular Oncology, New York, NY; David M. Gershenson, University of Texas MD Anderson Cancer Center, Houston, TX; and John Farley, St Joseph's Hospital and Medical Center, Phoenix, AZ.

Published online ahead of print at www.jco.org on August 31, 2015.

Processed as a Rapid Communication manuscript.

Support information appears at the end of this article.

Authors' disclosures of potential conflicts of interest are found in the article online at www.jco.org. Author contributions are found at the end of this article.

Corresponding author: Rachel Grisham, MD, Memorial Sloan Kettering Cancer Center, 1275 York Ave, New York, NY, 10065; e-mail: grishamr@mskcc.org.

0732-183X/15/3334w-4099w/$20.00

DOI: 10.1200/JCO.2015.62.4726

ABSTRACT

Purpose
No effective systemic therapy exists for patients with metastatic low-grade serous (LGS) ovarian cancers. *BRAF* and *KRAS* mutations are common in serous borderline (SB) and LGS ovarian cancers, and MEK inhibition has been shown to induce tumor regression in a minority of patients; however, no correlation has been observed between mutation status and clinical response. With the goal of identifying biomarkers of sensitivity to MEK inhibitor treatment, we performed an outlier analysis of a patient who experienced a complete, durable, and ongoing (> 5 years) response to selumetinib, a non-ATP competitive MEK inhibitor.

Patients and Methods
Next-generation sequencing was used to analyze this patient's tumor as well as an additional 28 SB/LGS tumors. Functional characterization of an identified novel alteration of interest was performed.

Results
Analysis of the extraordinary responder's tumor identified a 15-nucleotide deletion in the negative regulatory helix of the *MAP2K1* gene encoding for MEK1. Functional characterization demonstrated that this mutant induced extracellular signal-regulated kinase pathway activation, promoted anchorage-independent growth and tumor formation in mice, and retained sensitivity to selumetinib. Analysis of additional LGS/SB tumors identified mutations predicted to induce extracellular signal-regulated kinase pathway activation in 82% (23 of 28), including two patients with *BRAF* fusions, one of whom achieved an ongoing complete response to MEK inhibitor–based combination therapy.

Conclusion
Alterations affecting the mitogen-activated protein kinase pathway are present in the majority of patients with LGS ovarian cancer. Next-generation sequencing analysis revealed deletions and fusions that are not detected by older sequencing approaches. These findings, coupled with the observation that a subset of patients with recurrent LGS ovarian cancer experienced dramatic and durable responses to MEK inhibitor therapy, support additional clinical studies of MEK inhibitors in this disease.

J Clin Oncol 33:4099-4105. © 2015 by American Society of Clinical Oncology

INTRODUCTION

Serous epithelial ovarian, fallopian tube, and primary peritoneal tumors are classified using a two-tiered grading system into high- and low-grade serous (LGS) cancers.[1,2] LGS ovarian cancer accounts for 10% of serous ovarian cancers and is characterized by an early age of onset (median age, 46 years), slow growth pattern, and poor response to chemotherapy.[2,3] It is believed that many LGS cancers develop through a stepwise process that involves progression from benign serous borderline (SB) neoplasm to noninvasive micropapillary SB tumor and then to invasive LGS carcinoma.[4,5] The evidence for this stepwise progression is predominantly histologic, with little information currently available regarding the molecular drivers of progression from SB to LGS carcinoma.[3,6-8]

Prior molecular profiling studies have revealed that approximately two thirds of SB and LGS

ovarian tumors harbor mutations in the *BRAF* or *KRAS* gene.[9,10] The high prevalence of *BRAF* and *KRAS* mutations in LGS/SB tumors and the limited activity of cytotoxic agents in this disease prompted the evaluation of selective MEK inhibitors in patients with recurrent or metastatic LGS ovarian cancers.[7,8] A phase II study (GOG-239 [Gynecologic Oncology Group]) of single-agent selumetinib, a non-ATP competitive inhibitor of MEK1/2, in patients with recurrent LGS ovarian cancer reported a 15.4% radiographic response rate (partial or complete response [CR] by RECIST [version 1.1] criteria). No correlation was found between *BRAF* or *KRAS* mutation status and therapeutic response.[8]

To identify determinants of MEK inhibitor sensitivity in LGS ovarian cancer, we performed a genomic and functional outlier analysis of a patient who experienced a durable CR to selumetinib.

PATIENTS AND METHODS

Sample Collection and DNA Extraction

Tumor samples and matched blood were collected from 29 patients with LGS/SB ovarian cancer under an institutional review board–approved tissue collection protocol. Hematoxylin and eosin slides for all tumors were reviewed by an anatomic pathologist (D.D.) to confirm LGS/SB histology. Samples were macrodissected with the goal of exceeding 60% tumor content. DNA was extracted from frozen and paraffin-embedded samples using the DNeasy Tissue Kit (Qiagen, Valencia, CA).

Sequencing Methodology

Tumor and germline DNA were sequenced using the MSK-IMPACT (Memorial Sloan Kettering Integrated Mutation Profiling of Actionable Cancer Targets) assay, and sequence read alignment, processing, single-nucleotide variant, and copy number detections were performed as previously described.[11] Detection of somatic structural variants is described in the Appendix (online only).

A total of 42 LGS/SB samples were analyzed for *MAP2K1* alterations using a MiSeq platform (Illumina, San Diego, CA). After library preparation and adaptor ligation, barcoded DNA was hybridized to a flow cell and sequenced using paired-end primers.

Whole Transcriptome Analysis

After ribogreen quantification and quality control (Agilent BioAnalyzer; Agilent Technologies, Santa Clara, CA), polyA selection and Truseq library preparation were performed per manufacturer protocol (TruSeq RNA Sample Prep Kit [version 2]; Illumina), except for the following changes: mRNA strands were fragmented for 2 minutes, the adapter-ligated library was size selected (400 to 550 base pairs [bp]) with a Pippin prep (Sage Science, Beverly, MA), and the library was polymerase chain reaction amplified (10 cycles). Barcoded samples were sequenced in a 75-bp/75-bp paired-end run (TruSeq SBS Kit [version 3]; Illumina), generating 183 million paired reads. Ribosomal and mRNA reads represented 0.07% and 51%, respectively.

Functional Studies

Mutant *MAP2K1* constructs were generated from the MEK1–green fluorescent protein (GFP) plasmid (Cat. No. 14,746; Addgene, Cambridge, MA) using the QuickChange Site-Directed Mutagenesis Kit (Stratagene California, La Jolla, CA) and verified by Sanger sequencing. Using Lipofectamine 2000 (Invitrogen, Carlsbad, CA), 293H cells were transiently transfected with wild-type or mutant MEK1-GFP plasmid and standardized by GFP expression. Immunoblot analysis was performed as previously described.[12]

Dose-response studies. Cells were treated with 0.5, 1, or 2 μmol/L AZD6244 or dimethyl sulfoxide for 1 hour.

Retroviral infection. *MAP2K1* cDNA was subcloned from pEGFP-N1-MEK1-GFP into the MSCV-puro vector (Gateway; Invitrogen). NIH-3T3 cells were infected with retrovirus-containing medium and polybrene (Santa Cruz Biotechnology, Dallas, TX) for 48 hours. Cells were selected with puromycin for 7 days, followed by puromycin maintenance.

Colony formation studies. NIH-3T3 cells were plated over 0.5% agar on six-well plates, incubated at 37°C for 3 weeks, and stained with crystal violet (Sigma-Aldrich, St Louis, MO) for 1 hour at 37°C. Soft agar colonies were quantified using GelCount (Oxford Optronix, Abingdon, United Kingdom). Captured images were analyzed using uniform size and shape parameters.

In vivo studies. Athymic nude female mice age 6 to 8 weeks were maintained in compliance with Institutional Animal Care and Use Committee guidelines. Mice (five per cell line) underwent subcutaneous, double-flank injections of 8×10^6 NIH-3T3-MSCV-puro, NIH-3T3-MSCV-puro-MEK1, or mutant NIH-3T3-MSCV-puro-MEK1 cells in Matrigel (Corning Life Sciences, Corning, NY). Tumor growth was monitored three times per week for 3 weeks. All mice were euthanized and necropsied.

RESULTS

A 51-year-old patient with metastatic LGS ovarian cancer initially underwent optimal debulking for stage IIIC SB disease in 2005. She experienced recurrence with LGS ovarian cancer and progression with multiple lines of intravenous and intraperitoneal chemotherapy as well as tamoxifen. She was enrolled onto a phase II trial of selumetinib in 2009 (GOG-0239) and had achieved a CR by 2011 (Fig 1A). This response has been durable and ongoing (> 5 years) with continuous selumetinib therapy. This patient's tumor was screened for *KRAS* and *BRAF* mutations, performed using both polymerase chain reaction–based restriction fragment length polymorphism analysis and a mass spectrometry–based assay (Sequenom, San Diego, CA), neither of which revealed a hotspot alteration in either gene.

To explore the molecular basis for the patient's profound, durable response to MEK inhibition, we performed next-generation sequencing analysis of DNA derived from tumor tissue and germline DNA from blood. Using a capture-based platform (MSK-IMPACT), we assayed for alterations in 279 cancer-associated genes. This analysis confirmed that the tumor was *BRAF* and *KRAS* wild type but that it harbored a 15-bp in-frame deletion within the *MAP2K1* gene (Fig 1B). This deletion was identified in 60 (8.3%) of 725 sequence reads within the tumor and was absent in the germline DNA; it results in an in-frame deletion of five amino acids (p.Q56_V60del) adjacent to the negative regulatory helix of MEK1. The deletion was subsequently confirmed using an orthogonal validation assay (MiSeq; Illumina). Several recurrent, activating *MAP2K1* missense mutations have been identified either in proximity to or directly within the negative regulatory helix region, including F53L and K57N, respectively. The F53L mutation has been detected in lung and lymphoid cancers, whereas K57N has been confirmed as an oncogenic driver and has been identified in lung cancer, melanoma, and neuroblastoma (COSMIC [Catalogue of Somatic Mutations in Cancer] data[13-16]). Two in-frame deletions (F53_Q58delinsL and K57_G61del) within the helix A regulatory domain were recently reported in *BRAF* wild-type Langerhans histiocytosis.[17] These MEK1 alterations generally occur in a mutually exclusive distribution with G12 KRAS and V600E BRAF mutations, suggesting overlapping functional effects.

We used in silico three-dimensional modeling to predict the structural impact of the MEK1 Q56_V60 deletion (Fig 1C). This five–amino acid deletion results in the removal of the C-terminal portion of the negative regulatory helix, thereby shifting significantly the registration of the helix and positioning nonconservative amino

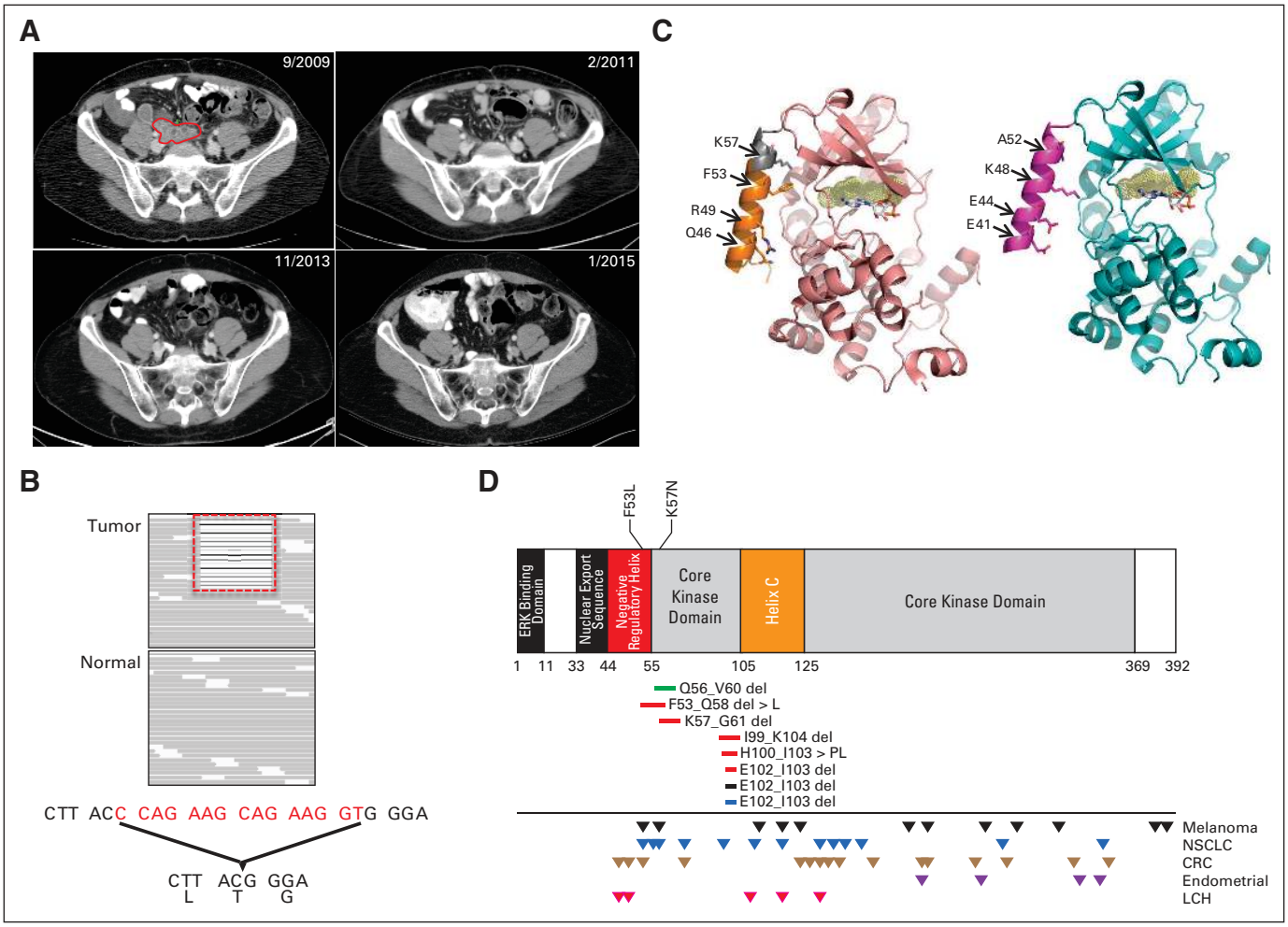

Fig 1. Analysis of extraordinary responder to selumetinib identifies 15–base pair deletion in *MAP2K1* gene. (A) Radiographic response of extraordinary responder to selumetinib therapy. Comparative computed tomography scan images at baseline and after treatment with selumetinib confirming complete radiographic response after 17 months of therapy, which was durable at 4 and 5 years. (B) *MAP2K1* deletion in outlier patient's tumor, as displayed using Integrated Genomics Viewer software (Broad Institute, Cambridge, MA). Sixty (8.3%) of 725 reads harbored deletion in tumor tissue, whereas no evidence of deletion was found in 434 reads from germline DNA derived from blood. Schematic below shows 15 nucleotides spanning six codons that were deleted, resulting in loss of five amino acids (QKQKV, underlined) within negative regulatory region of MEK1. (C) Two ribbon diagrams representing crystal structure of wild-type MEK1 on left and predicted structure of MEK1 Q56_V60 deletion on right. Deletion of residues 56 to 60 in MEK1 significantly alters interactions of inhibitory N-terminal helix A with the core kinase (right). In wild-type MEK1 structure, selected helix A residues that interact with core kinase are labeled as follows: MEK1 core kinase (pink), helix A (orange, with residues 56 to 60 in gray), allosteric inhibitor (gold), and guanosine diphosphate (GDP; white sticks). Consequent to deletion of five residues at C-terminus of helix A, registration of helix has shifted, resulting in nonconservative changes to helix A residues that interact with core kinase domain. In this predicted structure, the following are displayed: MEK1 core kinase (teal), truncated helix A (purple), allosteric inhibitor (yellow), and GDP (white sticks). (D) Schematic of MEK1 with alterations identified across cancer types is displayed. Major domains of protein are also shown. Horizontal bars below schematic represent deletions. Triangles represent point mutations and are distributed based on involved residue. Alterations displayed were chosen based on frequency of > 5% observed in COSMIC (Catalogue of Somatic Mutations in Cancer). CRC, colorectal cancer; ERK, extracellular signal-regulated kinase; LCH, Langerhans cell histiocytosis; NSCLC, non–small-cell lung cancer.

acid side chains near the core kinase domain. Consequently, the truncated helix is predicted to no longer pack tightly against the kinase domain, relieving its negative regulation on kinase activity. Notably, the allosteric inhibitor binding site of selumetinib is unaffected by this structural change. In Figure 1D, the location of the MEK1 Q56_V60 deletion is displayed with additional MEK1 alterations identified across multiple cancer types.

To elucidate the functional consequences of the MEK1 Q56_V60 deletion on mitogen-activated protein kinase (MAPK) signaling, we used site-directed mutagenesis to delete residues 56 to 60 of wild-type MEK1. Expression of the MEK1 Q56_V60 deletion as well as the previously characterized MEK1 F53L mutation in 293H cells resulted in significantly elevated levels of the MAPK pathway mediators phosphorylated extracellular signal-regulated kinase (ERK) and phosphorylated ribosomal protein S6 kinase (RSK) as compared with wild-type MEK1, confirming that both alterations are functionally active (Fig 2A). Exposure of MEK1-transfected cells to increasing concentrations of selumetinib for 1 hour followed by immunoblot analysis for phosphorylated ERK also confirmed that the MEK1 Q56_V60 deletion retained sensitivity to MEK inhibition (Fig 2B).

To gauge the transforming capability of the deletion, we measured anchorage-independent growth of NIH-3T3 cells after stable transfection with either wild-type MEK1, the F53L and K57N missense mutations, or the MEK1 Q56_V60 deletion.[14] As shown in Figure 2C, MEK1 Q56_V60 expression resulted in a significant increase in colony size and number when compared with vector alone

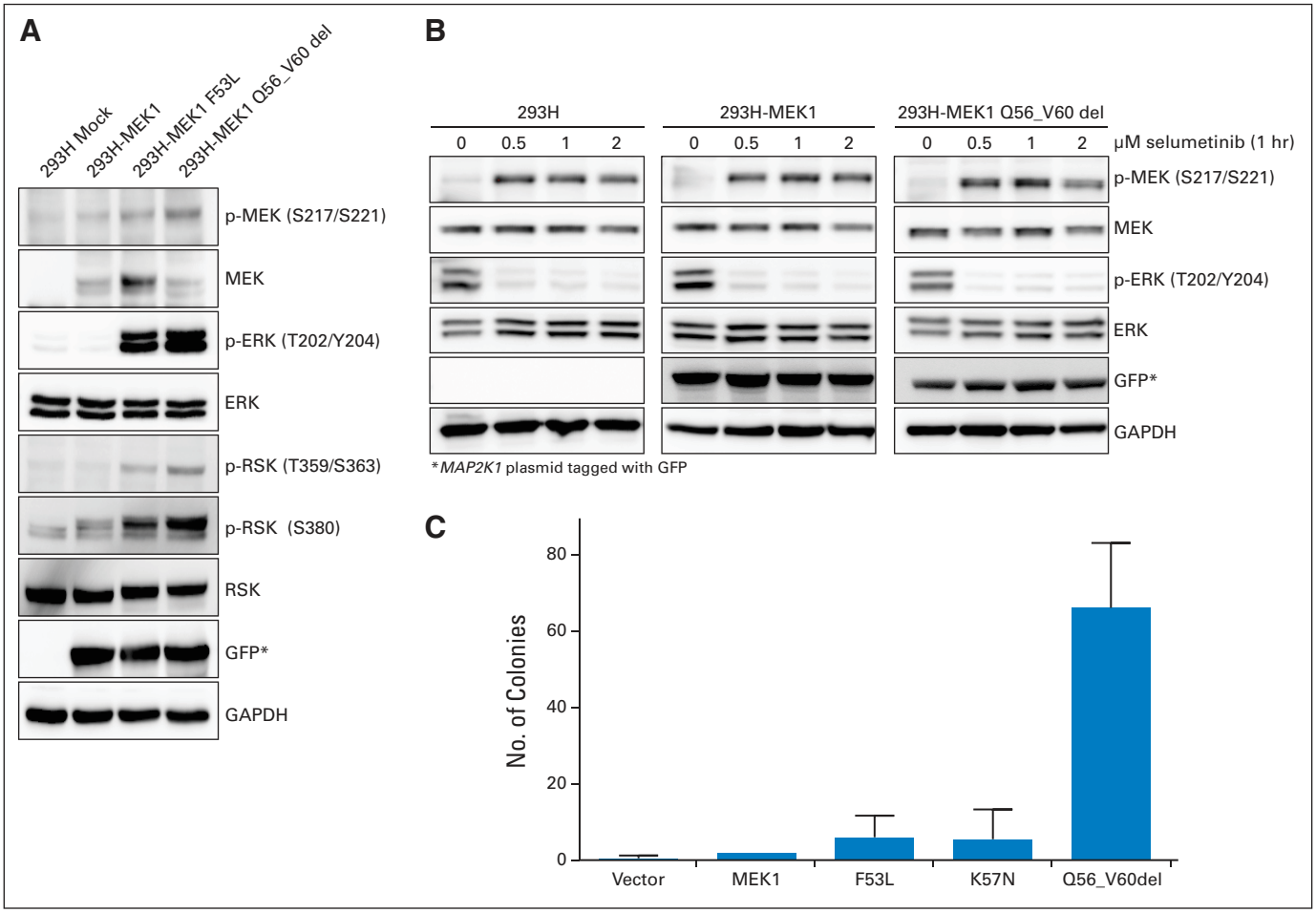

Fig 2. Functional characterization of MEK1 Q56_V60 deletion. (A) Immunoblots showing levels of phosphorylated MEK (pMEK), phosphorylated extracellular signal-regulated kinase (pERK), and phosphorylated ribosomal protein S6 kinase (pRSK) in 293H cells expressing MEK1 Q56_V60 deletion, MEK1 F53L, and wild-type MEK1. (B) Exposure to selumetinib of 293H cells expressing either wild-type MEK1 or MEK1 Q56_V60 deletion results in potent downregulation of pERK levels. (C) Soft agar colony formation assay after stable transfection of NIH-3T3 cells with vector alone, wild-type MEK1, two MEK1 oncogenic mutants (F53L and K57N), and MEK1 Q56_V60 deletion. Number of colonies resulting from MEK1 deletion was significantly increased as compared with vector ($P = .032$), wild-type MEK1, or F53L and K57N MEK1 mutants ($P = .045$). GAPDH, glyceraldehyde 3-phosphate dehydrogenase; GFP, green fluorescent protein.

($P = .032$) or the K57N mutation ($P = .045$). Furthermore, selumetinib treatment resulted in a dramatic inhibition of colony formation (Appendix Fig A1A, online only). To investigate the oncogenic effects of the deletion in vivo, nude mice were subcutaneously implanted in both flanks with stably infected NIH-3T3 cells expressing vector alone, wild-type MEK1, the F53L mutation, or the Q56_V60 deletion. Both MEK1 mutations induced a significant increase in the rate of tumor formation within 2 weeks of implantation versus a wild-type vector or uninfected cells (Appendix Fig A1B, online only).

To define the prevalence of *MAP2K1* mutations in LGS/SB tumors, all 11 exons in *MAP2K1* were sequenced in an additional 42 tumors (LGS, n = 14; SB, n = 28) using a MiSeq-based assay (Illumina); no *MAP2K1* deletions were identified in these samples. To determine whether other *BRAF*/*RAS* wild-type SB/LGS tumors harbored occult alterations in the MAPK pathway, we sequenced an additional 28 tumor samples (SB, n = 11; LGS, n = 17) using MSK-IMPACT (Fig 3A). The clinical characteristics and genetic alterations identified within each sample are listed in Appendix Table A1 (online only); sequencing metrics are listed in Appendix Table A2 (online only). The overall mutation rate was low, with an average of two alterations per sample, in keeping with prior reports that SB and LGS tumors are genomically quiescent.[18,19] Assessment of copy number alterations revealed focal *CDKN2A/B* deletions in two samples but no large-scale changes in chromosome structure or number. Consistent with previously published data, known activating *RAS* and *BRAF* mutations were common (occurring in 38% and 31% of samples, respectively) and mutually exclusive.[20,21] In The Cancer Genome Atlas analysis of high-grade serous ovarian tumors (n = 316), *KRAS* and *BRAF* alterations were significantly less frequent and *TP53* alterations much more common than in this SB/LGS cohort ($P < .001$; Fig 3B).

Several *RAS*/*BRAF* wild-type LGS samples harbored genetic alterations predicted to result in MAPK pathway signaling upregulation. Two samples harbored truncating mutations in the RAS GAP NF1, and a third sample harbored a 12-bp insertion in *ERBB2* (p.774_775insAYVM). This latter event results in an in-frame four–amino acid insertion within the human epidermal growth factor receptor 2 (HER2) kinase domain, which has been previously reported in non–small-cell lung cancer (NSCLC) and validated as an oncogenic activating mutation.[22] Two novel *BRAF* fusions were also identified in the LGS samples. One of these patients, who had been treated with

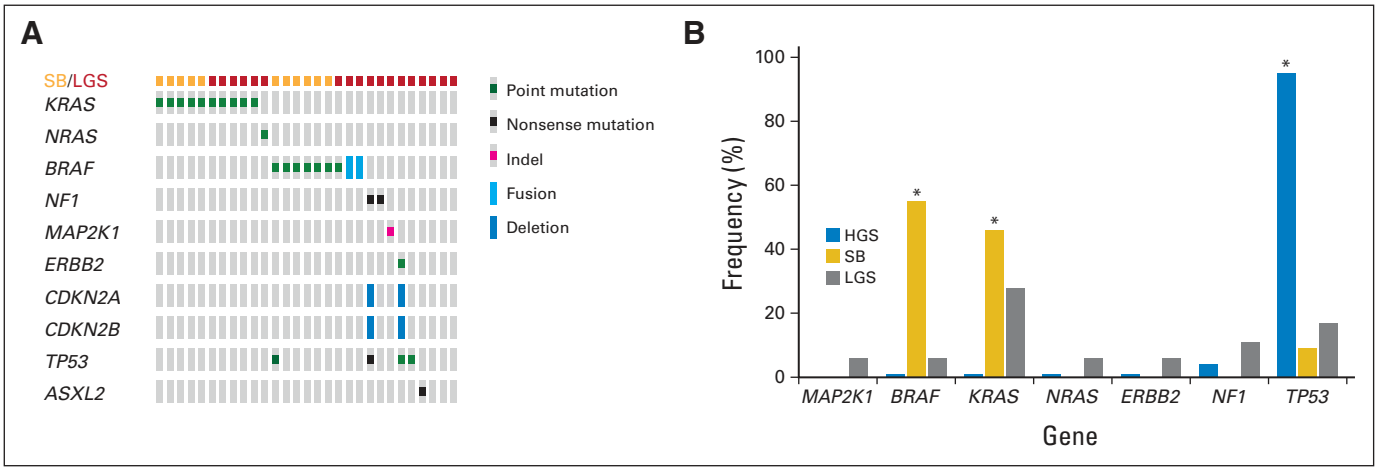

Fig 3. Low-grade serous (LGS)/serous borderline (SB) ovarian cancers are characterized by frequent mitogen-activated protein kinase pathway alterations. (A) Oncoprint displaying selected genetic alterations identified in cohort of 29 SB and LGS ovarian tumors. (B) Fisher's exact test was used to compare frequency of selected genetic alterations between 11 SB samples, 18 LGS ovarian tumors, and 316 high-grade serous (HGS) ovarian tumors analyzed by The Cancer Genome Atlas. (*) $P < .05$.

multiple lines of chemotherapy and hormonal therapy dating back to 1982, harbored an in-frame fusion involving the *BRAF* and *MKRN1* genes, the latter of which encodes for an E3 ubiquitin ligase. This fusion juxtaposes the first four exons of *MKRN1* with the *BRAF* kinase domain after an internal tandem duplication of this portion of chromosome 7 (Appendix Fig A2A, online only). A similar *MKRN1*:*BRAF* fusion was recently reported in pilocytic astrocytomas.[23] The second patient harbored a paracentric inversion within the long arm of chromosome 7, leading to an in-frame fusion between the BRAF kinase domain and the cullin protein, CUL1, a scaffolding component of the E3 ubiquitin ligase complex.[24] Whole-transcriptome sequencing confirmed expression of this fusion at the transcript level (Appendix Fig A2B, online only). Notably, this patient, who developed metastatic disease after treatment with carboplatin and paclitaxel, was enrolled onto a study of paclitaxel in combination with an oral MEK inhibitor and has since achieved a CR, with resolution of all sites of disease and normalization of serum cancer antigen 125 levels. She continued to receive therapy for 7 months, after which treatment was discontinued because of the development of pneumonitis. The patient has since been observed off treatment, with a sustained CR now lasting > 18 months.

DISCUSSION

Previous studies have reported hotspot mutations in *BRAF* and *KRAS* in approximately two thirds of patients with LGS/SB ovarian cancer. These results, along with the known sensitivity of *BRAF*-mutant tumors to MEK inhibition in preclinical models, prompted an open-label, single-arm phase II study of the MEK inhibitor selumetinib in patients with recurrent LGS ovarian cancer.[25] A 15.4% response rate was observed, with one patient achieving a CR. The presence of *BRAF* and *KRAS* alterations did not correlate with response to therapy; however, only hotspot mutations were assessed, and sufficient genetic material was available for analysis in only two thirds of patients.

To identify occult biomarkers of MEK inhibitor response in patients with LGS ovarian cancer, we performed an extreme outlier analysis of the single patient in GOG-0239 who achieved a CR. Historically, genetic analysis of LGS/SB tumors has been confounded by significant stromal infiltration and psammomatous calcifications. These features are common to most LGS/SB tumors, making mutation detection challenging using older methodologies. To overcome these technical hurdles, we employed an exon-capture sequencing platform to perform deep targeted sequencing of known cancer genes to a target coverage of > 500-fold depth. Analysis of the extraordinary responder identified a previously uncharacterized *MAP2K1* deletion. In silico structural modeling of this deletion (Q56_V60del) predicted that it would disrupt the interaction between the negative regulatory helix and the core kinase domain, resulting in constitutive kinase activation. In support of this model, expression of MEK1 Q56_V60del in 293H cells engendered increased expression of downstream effectors of MEK, including phosphorylated ERK and RSK, which were potently inhibited after selumetinib treatment. Cells expressing MEK1 Q56_V60del displayed enhanced colony formation in soft agar as compared with both wild-type MEK1 and two previously reported recurrent missense MEK1 mutations. Furthermore, MEK1 Q56_V60 deletion was associated with enhanced tumor formation in mice compared with empty-vector or wild-type MEK1. In summary, these results provide compelling support that MEK1 Q56_V60 deletion is a driver alteration in the index extraordinary responder and that this mutation serves as the molecular basis for her dramatic, sustained response to selumetinib.

Activating MEK1 mutations have been identified in a variety of tumor types. K57N, the most frequently reported mutation, was first reported in NSCLC but has subsequently been detected in melanoma, head and neck cancer, and prostate cancer.[26] Functional characterization of this mutant in vitro demonstrated constitutive activation of ERK signaling, cytokine-independent growth, and sensitivity to selumetinib.[14] The F53L mutation has been reported in melanoma and colorectal, lung, and gastric cancers,[26] and genomic and functional studies have confirmed that this mutant represents a basis for acquired resistance to combined RAF/MEK inhibitors.[27] Other mutations in MEK1, including an in-frame deletion at K59, have also been

associated with resistance to BRAF inhibitors.[28] Both K57N and F53L, along with the Q56_V60 deletion mutation, cluster in the negative regulatory region (near helix A) of MEK1. Helix A is an extension of the N terminus and is unique to the MEK protein family. It contacts the N-terminal lobe of the MEK core kinase domain and is predicted to act as a clamp, locking the active center of the kinase domain (helix C) into a closed conformation, suppressing MEK enzymatic activity. Our modeling predicts that all three mutants affect the tertiary structure of inactive MEK1 by disruption of side-chain interactions between the negative regulatory region and the kinase domain, leading to an open conformational state.

Because the index extraordinary responder harbored a mutation resulting in MAPK pathway activation, we screened additional LGS/SB tumors to assess whether alterations predicted to induce ERK activation were common in the *KRAS*/*BRAF* wild-type cohort. NGS analysis of 28 additional samples confirmed that activating *BRAF* and *KRAS* mutations are common in LGS/SB tumors and that these tumors have a low somatic mutation burden.[20,21,29,30] Although no additional MEK1 deletions were detected, alterations predicted to induce MAPK pathway activation were identified in five of 10 *BRAF/KRAS* wild-type tumors: two truncating mutations in the RAS GAP NF1, one NRAS Q61R mutation, one HER2 AYVM insertion, and two *BRAF* paracentric fusions. The AYVM insertion is the most common activating HER2 alteration in NSCLC. Both the *MKRN1*:*BRAF* and *CUL1*:*BRAF* fusions are in frame and result in loss of the RAS binding domain of *BRAF*. This is predicted to lead to constitutive kinase activation.[31] Notably, the *CUL1*:*BRAF* fusion was detected in a patient who experienced a sustained CR to MEK inhibitor therapy in combination with paclitaxel. Both the MEK1 deletion and the *BRAF* fusion may result in greater dependence on an activated MAPK pathway for growth and survival than *KRAS* mutations, which potentially activate other mitogenic pathways, such as the phosphatidylinositol 3-kinase pathway. The observation that MEK inhibitors were effective in only a subset of patients with MAPK pathway alterations in GOG-0239 is consistent with prior results in other cancer types, including melanoma.[32] The molecular basis for this heterogeneity of response to MEK inhibition remains unknown but may in part result from variation in the pattern of co-mutated genes.[33] Because LGS ovarian cancer typically lacks co-mutations found to diminish MEK dependence, response to MAPK pathway inhibitors in patients with this disease may prove to be more durable than in patients with highly mutated cancers, such as melanoma.

The detection of multiple, distinct genetic alterations in a mutually exclusive pattern within the MAPK pathway suggests that dysregulated MAPK signaling is likely a hallmark of most, if not all, SB/LGS ovarian cancers. In our analysis, we failed to identify MAPK pathway alterations in only five tumors (17%). These samples may harbor noncanonic MAPK pathway–activating alterations that were not detectable by our exon-capture assay. Alternatively, a subset of SB/LGS tumors may exist in which ERK activation does not contribute to tumor initiation or progression. Broader whole-genome and -transcriptome studies of such wild-type patients may identify additional somatic drivers that induce MAPK pathway activation. Interestingly, the patients with exceptional responses harbored novel alterations affecting the MAPK pathway, as opposed to hotspot *KRAS* or *BRAF* mutations. Our findings explain why targeted genotyping of only the most common hotspot alterations in *BRAF* and *KRAS* failed to ascertain the molecular basis for a subset of the responses observed on GOG-0239 and justify the incorporation of broader profiling methods into ongoing and future clinical trials of patients with LGS cancer.

In summary, we find that almost all patients with SB/LGS ovarian cancer harbor a mutation predicted to induce ERK activation. These results support continued studies of MEK and ERK inhibitors in patients with LGS tumors and in MEK1-mutant patients more broadly.

AUTHORS' DISCLOSURES OF POTENTIAL CONFLICTS OF INTEREST

Disclosures provided by the authors are available with this article at www.jco.org.

AUTHOR CONTRIBUTIONS

Conception and design: Rachel N. Grisham, David M. Gershenson, John Farley, David R. Spriggs, Carol Aghajanian, David B. Solit, Gopa Iyer
Provision of study materials or patients: Evis Sala
Collection and assembly of data: Rachel N. Grisham, Brooke E. Sylvester, Helen Won, Gregory McDermott, Deborah DeLair, Ricardo Ramirez, Zhan Yao, Ronglai Shen, Fanny Dao, Faina Bogomolniy, Vicky Makker, Evis Sala, Nicholas D. Socci, Agnes Viale, Douglas A. Levine, Michael F. Berger, David B. Solit, Gopa Iyer
Data analysis and interpretation: Rachel N. Grisham, Brooke E. Sylvester, Helen Won, Gregory McDermott, Deborah DeLair, Ricardo Ramirez, Zhan Yao, Ronglai Shen, Fanny Dao, Faina Bogomolniy, Vicky Makker, Evis Sala, David M. Hyman, Nicholas D. Socci, Agnes Viale, David M. Gershenson, John Farley, Douglas A. Levine, Neal Rosen, Michael F. Berger, David R. Spriggs, Carol Aghajanian, David B. Solit, Gopa Iyer
Manuscript writing: All authors
Final approval of manuscript: All authors

REFERENCES

1. Bodurka DC, Deavers MT, Tian C, et al: Reclassification of serous ovarian carcinoma by a 2-tier system: A Gynecologic Oncology Group Study. Cancer 118:3087-3094, 2012
2. Vang R, Shih IeM, Salani R, et al: Subdividing ovarian and peritoneal serous carcinoma into moderately differentiated and poorly differentiated does not have biologic validity based on molecular genetic and in vitro drug resistance data. Am J Surg Pathol 32:1667-1674, 2008
3. Schmeler KM, Sun CC, Bodurka DC, et al: Neoadjuvant chemotherapy for low-grade serous carcinoma of the ovary or peritoneum. Gynecol Oncol 108:510-514, 2008
4. Russell SE, McCluggage WG: A multistep model for ovarian tumorigenesis: The value of mutation analysis in the KRAS and BRAF genes. J Pathol 203:617-619, 2004
5. Smith Sehdev AE, Sehdev PS, Kurman RJ: Noninvasive and invasive micropapillary (low-grade) serous carcinoma of the ovary: A clinicopathologic analysis of 135 cases. Am J Surg Pathol 27:725-736, 2003
6. Gershenson DM, Sun CC, Bodurka D, et al: Recurrent low-grade serous ovarian carcinoma is relatively chemoresistant. Gynecol Oncol 114:48-52, 2009
7. Bedard P, Tabernero J, Kurzrock R, et al: A phase Ib,open-label, multicenter, dose-escalation study of the oral pan-PI3K inhibitor BKM120 in combination with the oral MEK1/2 inhibitor GSK1120212 in patients (pts) with selected advanced solid tumors. J Clin Oncol 30:173s, 2012 (suppl 15s; abstr 3003)
8. Farley J, Brady WE, Vathipadiekal V, et al: Selumetinib in women with recurrent low-grade

serous carcinoma of the ovary or peritoneum: An open-label, single-arm, phase 2 study. Lancet Oncol 14:134-140, 2013

9. Ho CL, Kurman RJ, Dehari R, et al: Mutations of BRAF and KRAS precede the development of ovarian serous borderline tumors. Cancer Res 64: 6915-6918, 2004

10. Singer G, Oldt R 3rd, Cohen Y, et al: Mutations in BRAF and KRAS characterize the development of low-grade ovarian serous carcinoma. J Natl Cancer Inst 95:484-486, 2003

11. Kim PH, Cha EK, Sfakianos JP, et al: Genomic predictors of survival in patients with high-grade urothelial carcinoma of the bladder. Eur Urol 67:198-201, 2015

12. Pratilas CA, Taylor BS, Ye Q, et al: (V600E) BRAF is associated with disabled feedback inhibition of RAF-MEK signaling and elevated transcriptional output of the pathway. Proc Natl Acad Sci U S A 106:4519-4524, 2009

13. Rossi D, Trifonov V, Fangazio M, et al: The coding genome of splenic marginal zone lymphoma: Activation of NOTCH2 and other pathways regulating marginal zone development. J Exp Med 209: 1537-1551, 2012

14. Marks JL, Gong Y, Chitale D, et al: Novel MEK1 mutation identified by mutational analysis of epidermal growth factor receptor signaling pathway genes in lung adenocarcinoma. Cancer Res 68: 5524-5528, 2008

15. Murugan AK, Dong J, Xie J, et al: MEK1 mutations, but not ERK2 mutations, occur in melanomas and colon carcinomas, but none in thyroid carcinomas. Cell Cycle 8:2122-2124, 2009

16. Shukla N, Ameur N, Yilmaz I, et al: Oncogene mutation profiling of pediatric solid tumors reveals significant subsets of embryonal rhabdomyosarcoma and neuroblastoma with mutated genes in growth signaling pathways. Clin Cancer Res 18:748-757, 2012

17. Brown NA, Furtado LV, Betz BL, et al: High prevalence of somatic MAP2K1 mutations in BRAF V600E-negative Langerhans cell histiocytosis. Blood 124:1655-1658, 2014

18. Boyd J, Luo B, Peri S, et al: Whole exome sequence analysis of serous borderline tumors of the ovary. Gynecol Oncol 130:560-564, 2013

19. Jones S, Wang TL, Kurman RJ, et al: Low-grade serous carcinomas of the ovary contain very few point mutations. J Pathol 226:413-420, 2012

20. Grisham RN, Iyer G, Garg K, et al: BRAF mutation is associated with early stage disease and improved outcome in patients with low-grade serous ovarian cancer. Cancer 119:548-554, 2013

21. Wong KK, Tsang YT, Deavers MT, et al: BRAF mutation is rare in advanced-stage low-grade ovarian serous carcinomas. Am J Pathol 177:1611-1617, 2010

22. Perera SA, Li D, Shimamura T, et al: HER2YVMA drives rapid development of adenosquamous lung tumors in mice that are sensitive to BIBW2992 and rapamycin combination therapy. Proc Natl Acad Sci U S A 106:474-479, 2009

23. Jones DT, Hutter B, Jäger N, et al: Recurrent somatic alterations of FGFR1 and NTRK2 in pilocytic astrocytoma. Nat Genet 45:927-932, 2013

24. Pintard L, Willis JH, Willems A, et al: The BTB protein MEL-26 is a substrate-specific adaptor of the CUL-3 ubiquitin-ligase. Nature 425:311-316, 2003

25. Solit DB, Garraway LA, Pratilas CA, et al: BRAF mutation predicts sensitivity to MEK inhibition. Nature 439:358-362, 2006

26. Gao J, Aksoy BA, Dogrusoz U, et al: Integrative analysis of complex cancer genomics and clinical profiles using the cBioPortal. Sci Signal 6:pl1, 2013

27. Ahronian LG, Sennott EM, Van Allen EM, et al: Clinical acquired resistance to RAF inhibitor combinations in BRAF-mutant colorectal cancer through MAPK pathway alterations. Cancer Discov 5:358-367, 2015

28. Greger JG, Eastman SD, Zhang V, et al: Combinations of BRAF, MEK, and PI3K/mTOR inhibitors overcome acquired resistance to the BRAF inhibitor GSK2118436 dabrafenib, mediated by NRAS or MEK mutations Mol Cancer Ther 11:909-920, 2012

29. Tsang YT, Deavers MT, Sun CC, et al: KRAS (but not BRAF) mutations in ovarian serous borderline tumour are associated with recurrent low-grade serous carcinoma. J Pathol 231:449-456, 2013

30. Cancer Genome Atlas Research Network: Integrated genomic analyses of ovarian carcinoma. Nature 474:609-615, 2011

31. Hutchinson KE, Lipson D, Stephens PJ, et al: BRAF fusions define a distinct molecular subset of melanomas with potential sensitivity to MEK inhibition. Clin Cancer Res 19:6696-6702, 2013

32. Flaherty KT, Robert C, Hersey P, et al: Improved survival with MEK inhibition in BRAF-mutated melanoma. N Engl J Med 367:107-114, 2012

33. Xing F, Persaud Y, Pratilas CA, et al: Concurrent loss of the PTEN and RB1 tumor suppressors attenuates RAF dependence in melanomas harboring (V600E)BRAF. Oncogene 31:446-457, 2012

Support

Supported by Cycle for Survival, the Laura Mercier Ovarian Cancer Fund, the Kaleidoscope of Hope Foundation, and a Liz Tilberis Early Career Award provided by the Ovarian Cancer Research Fund (R.N.G.); by the Starr Foundation; by the Marie-Josée and Henry R. Kravis Center for Molecular Oncology; and in part by the Integrated Genomics Operation Core, funded by National Cancer Institute Cancer Center Core Grant No. P30 CA008748 (core grant provides funding to institutional cores [eg, biostatistics], which was used in this study). D.M.G. is supported by SPORE in Ovarian Cancer Grant No. P5083639.

AUTHORS' DISCLOSURES OF POTENTIAL CONFLICTS OF INTEREST

Extreme Outlier Analysis Identifies Occult Mitogen-Activated Protein Kinase Pathway Mutations in Patients With Low-Grade Serous Ovarian Cancer

The following represents disclosure information provided by authors of this manuscript. All relationships are considered compensated. Relationships are self-held unless noted. I = Immediate Family Member, Inst = My Institution. Relationships may not relate to the subject matter of this manuscript. For more information about ASCO's conflict of interest policy, please refer to www.asco.org/rwc or jco.ascopubs.org/site/ifc.

Rachel N. Grisham
Consulting or Advisory Role: Amgen
Travel, Accommodations, Expenses: Medivation/Astellas

Brooke E. Sylvester
No relationship to disclose

Helen Won
No relationship to disclose

Gregory McDermott
No relationship to disclose

Deborah DeLair
No relationship to disclose

Ricardo Ramirez
No relationship to disclose

Zhan Yao
No relationship to disclose

Ronglai Shen
No relationship to disclose

Fanny Dao
No relationship to disclose

Faina Bogomolniy
No relationship to disclose

Vicky Makker
No relationship to disclose

Evis Sala
No relationship to disclose

Tara E. Soumerai
No relationship to disclose

David M. Hyman
Consulting or Advisory Role: Atara Biotherapeutics, Chugai Pharmaceutical
Patents, Royalties, Other Intellectual Property: Patent No. PCT/US2014/061281 for detecting and monitoring mutations in histiocytosis
Travel, Accommodations, Expenses: Puma Biotechnology, Roche/Genentech

Nicholas D. Socci
No relationship to disclose

Agnes Viale
No relationship to disclose

David M. Gershenson
Stock or Other Ownership: Johnson & Johnson, Proctor and Gamble, Biogen Idec
Patents, Royalties, Other Intellectual Property: Royalties from Elsevier, UpToDate

John Farley
Consulting or Advisory Role: Genentech
Speakers' Bureau: Genentech

Douglas A. Levine
Consulting or Advisory Role: Boerhinger Ingelheim

Neal Rosen
No relationship to disclose

Michael F. Berger
Consulting or Advisory Role: Cancer Genetics, Sequenom

David R. Spriggs
Patents, Royalties, Other Intellectual Property: Through my laboratory, we have discovered anti-MUC16 antibodies about which Memorial Sloan Kettering Cancer Center has filed patents; these patents, if commercialized, could ultimately result in royalties paid to me (Inst)

Carol Aghajanian
Consulting or Advisory Role: AstraZeneca
Travel, Accommodations, Expenses: AstraZeneca, Abbvie

David B. Solit
Honoraria: Novartis, Loxo Oncology, Pfizer
Consulting or Advisory Role: Novartis, Pfizer, Loxo Oncology

Gopa Iyer
No relationship to disclose

Acknowledgment

We thank Barb Brandhuber, PhD, for her assistance with modeling of the structural effects of the MEK1 deletion.

Appendix

Methods

For *CUL1*:*BRAF* fusion detection, somatic structural variants were detected by Geometric Analysis of Structural Variants software (http://cs.brown.edu/people/braphael/software.html) using matched normal read-pair data. Potential rearrangements were identified with at least five paired or split reads at lengths > 1,000 base pairs. Candidate rearrangements were manually reviewed using Integrative Genomics Viewer software (Broad Institute, Cambridge, MA). The fusion was confirmed using Sanger sequencing of polymerase chain reaction–amplified products spanning breakpoint sites. The *MKRN1*:*BRAF* fusion was identified using DELLY software (version 0.3.3; www.korbel.embl.de/software.html) to detect somatic structural variants from tumor and matched normal read-pair data. The following supporting evidence was required: five paired or split reads, mapping quality > 20, and length > 500 base pairs. All candidate somatic rearrangements were filtered, annotated, and manually reviewed using Integrative Genomics Viewer. For MiSeq analysis, 42 low-grade serous/serous borderline samples were analyzed for *MAP2K1* alterations using a MiSeq platform (Illumina, San Diego, CA). After library preparation and adaptor ligation, barcoded DNA was hybridized to a flow cell and sequenced using paired-end primers.

Table A1. Characteristics of SB and LGS Tumors and Alterations Identified (N = 29)

Sample	Disease Stage	Histology	Arising in SB	Prior Therapies for Disease	Current Status	Mutation	Allele Frequency
RG-1	IIIC	LGS	Yes	IV carboplatin/paclitaxel IP paclitaxel/IV bevacizumab Tamoxifen AZD6244	NED	MEK1 p.Q56_V60del	0.08
RG-2	IIIC	SB	No	None	NED	KRAS G12V	0.37
						CDH1 p.10-11AL>V	0.09
						CDH11 T255M	0.10
						HNF1A I27L	0.08
						IL7R T244I	0.08
						NOTCH2 P6fs	0.18
						NOTCH4 K177Q	0.12
RG-3	IC	SB	No	None	NED	BRAF V600E	0.50
						MAP3K8 A191V	0.27
						RB1 S758L	0.08
RG-4	IIIC	LGS	Yes	IV carboplatin/paclitaxel Weekly paclitaxel Topotecan IV cisplatin	Dead	ALK p.1073_1075LQS>R	0.29
						CDKN2A deletion	
						CDKN2B deletion	
						CIC A796T	0.71
						HER2 p.774_775insAYVM	0.11
						TP53 R248W	0.07
RG-5	IIIC	LGS	Yes	IV carboplatin/paclitaxel IV gemcitabine/paclitaxel IV liposomal doxorubicin	Dead	*CDKN2A* deletion	
						CDKN2B deletion	
						NF1 Q803_splice	0.70
						TP53 S99fs	0.69
RG-6	IIC	SB	No	None	NED	BRAF V600E	0.27
						TP53 R248W	0.10
RG-7	IIIC	LGS	Yes	IV gemcitabine/IP cisplatin IV liposomal doxorubicin IV carboplatin Exemestane IV topotecan IV bevacizumab/oral cyclophosphamide IV gemcitabine IV carboplatin IV vinorelbine Oral etoposide Lupron	Dead	KRAS G12R	0.52

(continued on following page)

Table A1. Characteristics of SB and LGS Tumors and Alterations Identified (N = 29) (continued)

Sample	Disease Stage	Histology	Arising in SB	Prior Therapies for Disease	Current Status	Mutation	Allele Frequency
RG-8	IIIC	LGS	Yes	IV carboplatin/paclitaxel	NED	*CUL1:BRAF* fusion	
				IV paclitaxel/MEK162		XPO1 M7V	0.36
RG-9	IIIC	LGS	No	IV carboplatin/paclitaxel IV carboplatin/gemcitabine E7389 IV liposomal doxorubicin IV topotecan IV cisplatin Tamoxifen Letrozole IV paclitaxel	Dead	TP53 R248W	0.06
RG-10	IA	LGS	Yes	None	NED	BRAF V600E	0.47
RG-11	IA	SB	No	None	NED	BRAF V600E	0.08
RG-12	IIIC	LGS	Yes	IV paclitaxel/IP cisplatin/IP paclitaxel IV carboplatin/liposomal doxorubicin IV paclitaxel/bevacizumab	Active disease	KRAS G12V	0.52
RG-13	IIIC	LGS	Yes	IV carboplatin/paclitaxel IV paclitaxel/IP cisplatin Abagovomab or placebo Letrozole IV liposomal doxorubicin/carboplatin IV bevacizumab/oral cyclophosphamide IV bevacizumab/paclitaxel Tamoxifen IV bevacizumab/carboplatin IV bevacizumab	Active disease	ASXL1 P582fs	0.27
RG-14	IIIB	SB	No	IV carboplatin/paclitaxel	NED	KRAS G12D	0.25
RG-15	IIIC	LGS	Yes	IV paclitaxel/IP cisplatin/IP paclitaxel IV carboplatin/IV liposomal doxorubicin	Active disease	None	
RG-16	IIIC	SB	No	None	NED	KRAS G12V	0.46
RG-17	IIIC	LGS	Yes	IV paclitaxel/IP cisplatin/IP paclitaxel Letrozole	NED	KRAS G12V	0.25
RG-18	IC	SB	No	None	NED	BRAF V600E	0.27
RG-19	IA	SB	No	None	NED	KRAS G12D	0.17
RG-20	IC	SB	No	None	NED	BRAF V600E	0.18
RG-21	IA	SB	No	None	NED	KRAS G12D	0.66
RG-22	IA	SB	No	None	NED	BRAF V600E	0.12
						NOTCH2 P6fs	0.13
				IV paclitaxel/IP cisplatin/IP paclitaxel		NRAS Q61R	0.14
				IV liposomal doxorubicin/carboplatin		EIF1AX G9V	0.09
RG-23	IIIC	LGS	No	Tamoxifen Exemestane	Active disease	CTCF T518S	0.07
RG-24	IC	LGS	Yes	Unknown chemotherapy Letrozole Tamoxifen IV carboplatin/paclitaxel Exemestane	Active disease	*MKRN1:BRAF* fusion	
RG-25	IIIC	LGS	No	IV paclitaxel/IP cisplatin/IP paclitaxel IV bevacizumab/oral cyclophosphamide SAR245409/MSC1936369B MEDI-3617 Liposomal doxorubicin PU-H71 Iso-fludelone Carboplatin Letrozole	Dead	None	
RG-26	IIIC	LGS	Yes	Carboplatin	Active disease	KRAS G12V	0.62
				IV paclitaxel/IP cisplatin/IP paclitaxel		KRAS G12V	0.45
				IV carboplatin/gemcitabine		PDGFRB G607S	0.14

(continued on following page)

Table A1. Characteristics of SB and LGS Tumors and Alterations Identified (N = 29) (continued)

Sample	Disease Stage	Histology	Arising in SB	Prior Therapies for Disease	Current Status	Mutation	Allele Frequency
RG-27	IIIC	LGS	No	Letrozole MEK162	Active disease	*SOX17* amplification	
RG-28	IIIC	LGS	No	IV carboplatin/paclitaxel	Active disease	None	
RG-29	IIIC	LGS	Yes	IV paclitaxel/IP cisplatin/IP paclitaxel Abagovomab or placebo IV carboplatin/paclitaxel Liposomal doxorubicin	Active disease	NF1 P890fs	0.58

NOTE. Clinical characteristics and genomic alterations identified by MSK-IMPACT (Memorial Sloan Kettering Integrated Mutation Profiling of Actionable Cancer Targets).
Abbreviations: IP, intraperitoneal; IV, intravenous; LGS, low-grade serous; NED, no evidence of disease; SB, serous borderline.

Table A2. Sequencing Metrics for All Samples (N = 29)

Sample	Fold Coverage	Exons > 100× Coverage (%)	Average Insert Size (bp)
RG-1T	575	98.7	127
RG-1N	270	97.0	153
RG-2T	144	92.1	121
RG-2N	254	96.9	144
RG-3T	232	97.2	120
RG-3N	578	98.4	146
RG-4T	510	96.8	125
RG-4N	302	96.2	142
RG-5T	595	97.5	126
RG-5N	646	98.7	145
RG-6T	491	97.0	125
RG-6N	556	98.7	148
RG-7T	301	97.6	123
RG-7N	500	98.6	141
RG-8T	526	97.4	128
RG-8N	443	98.2	150
RG-9T	386	96.7	121
RG-9N	363	97.3	143
RG-10T	455	98.9	119
RG-10N	438	98.4	144
RG-11T	320	97.9	122
RG-11N	223	96.7	145
RG-12T	603	98.3	125
RG-12N	302	97.4	138
RG-13T	505	97.8	125
RG-13N	425	98.3	148
RG-14T	370	96.2	130
RG-14N	485	98.6	148
RG-15T	398	98.6	123
RG-15N	333	97.4	146
RG-16T	755	97.9	133
RG-16N	373	97.9	142
RG-17T	256	98.5	120
RG-17N	269	97.3	145
RG-18T	695	98.8	133
RG-18N	400	98.0	155
RG-19T	254	97.5	126
RG-19N	269	97.2	143
RG-20T	456	97.4	138
RG-20N	323	97.1	152
RG-21T	200	91.7	118
RG-21N	496	98.6	145
RG-22T	648	98.6	133
RG-22N	459	98.1	144
RG-23T	376	98.3	126
RG-23N	272	97.7	151
RG-24T	115	77.1	132
RG-24N	300	97.9	152
RG-25T	553	98.4	125
RG-25N	444	98.1	165
RG-26T	827	98.7	121
RG-26N	513	98.4	123
RG-27T	379	97.9	119
RG-27N	587	98.0	139
RG-28T	609	98.5	125
RG-28N	477	98.4	148
RG-29T	532	98.5	131
RG-29N	513	98.3	152

Abbreviations: bp, base pair; N, matched normal sample; T, tumor.

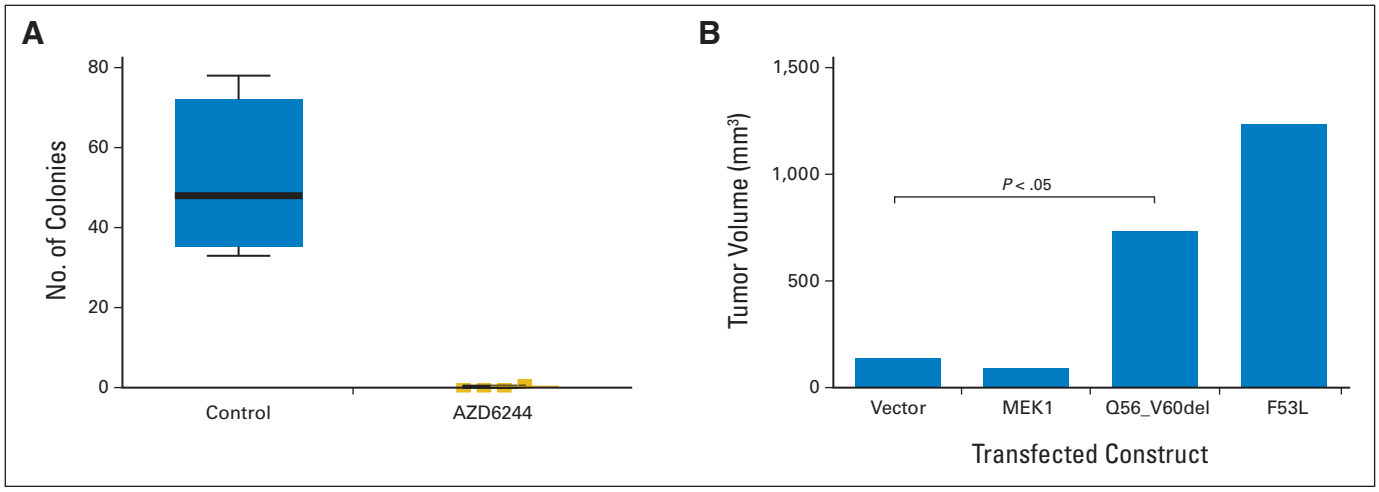

Fig A1. *MEK1* Q56_V60 deletion induces anchorage-independent growth in vitro and accelerates tumor growth in xenograft models. (A) Colony growth in soft agar of NIH-3T3 cells transfected with *MEK1* Q56_V60 deletion in presence or absence of AZD6244. (B) Tumor volume of xenografts generated by transfection of NIH-3T3 cells with empty vector, wild-type *MEK1*, *MEK1* Q56_V60 deletion, or *MEK1* F53L. Measurements were taken at day 11 postimplantation.

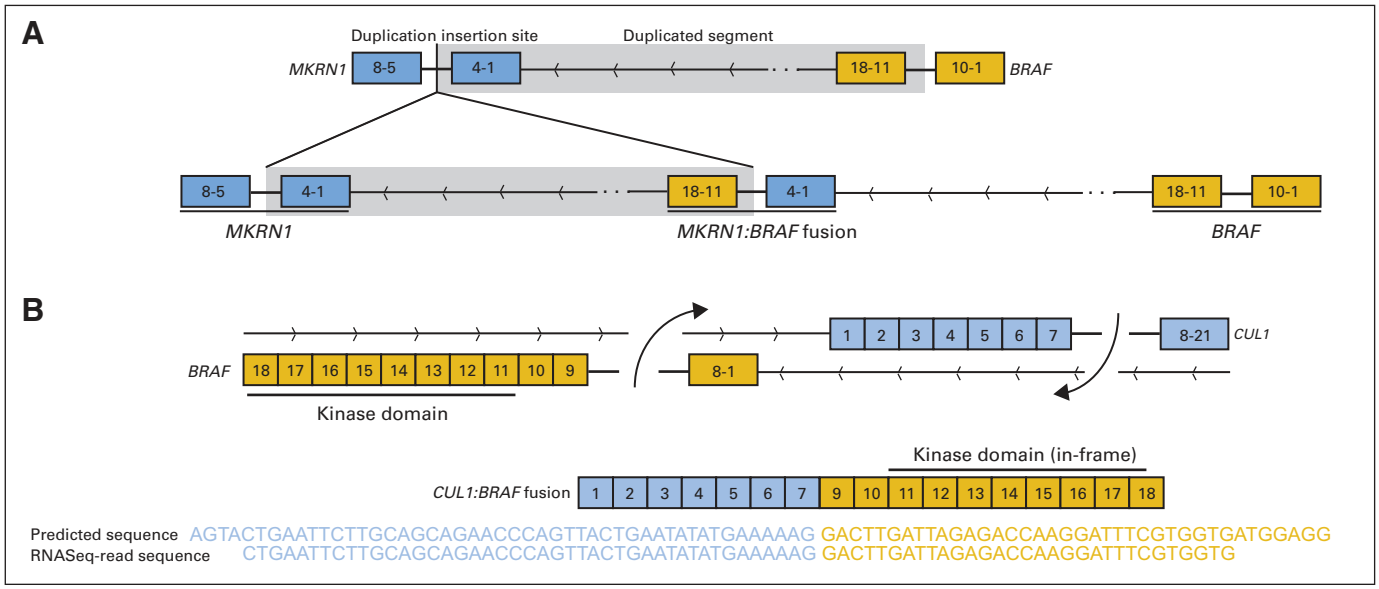

Fig A2. Schematic of two novel paracentric fusions involving *BRAF* in low-grade serous tumors. (A) To form *MKRN1:BRAF* fusion, internal tandem duplication of region of chromosome 7 containing exons 1 to 4 of *MKRN1* (blue) and exons 11 to 18 of *BRAF* (gold) occurs first (shaded box), followed by insertion of this region into intron 4 of *MKRN1*, juxtaposing exons 1 to 4 of *MKRN1* and exons 11 to 18 of *BRAF* (kinase domain). (B) Schematic of paracentric inversion in chromosome 7, which results in *CUL1:BRAF* fusion. *CUL1* and *BRAF* are located on sense and antisense strands, respectively. After breakpoint occurs within exon 7 of *CUL1* and exon 8 of *BRAF*, this region undergoes inversion, leading to juxtaposition of exons 1 to 7 of *CUL1* and exons 9 to 18 (containing intact kinase domain) of *BRAF*. Representative sequences from RNA sequencing of tumor harboring fusion are shown below.